

**SIMULATED KWAJEX CONVECTIVE SYSTEMS
USING A 2D AND 3D CLOUD RESOLVING MODEL
AND THEIR COMPARISONS WITH RADAR OBSERVATIONS**

Chung-Lin Shie^{1,2}, Wei-Kuo Tao¹, and Joanne Simpson¹

¹Laboratory for Atmospheres
NASA/Goddard Space Flight Center, Greenbelt, MD 20771

²Goddard Earth Sciences and Technology Center
University of Maryland, Baltimore County, Baltimore, MD 21250

1. INTRODUCTION

Cloud resolving model (CRM) has widely been used in recent years for simulations involving studies of radiative-convective systems and their role in determining the tropical regional climate. The growing popularity of CRMs usage can be credited for their inclusion of crucial and realistic features such as explicit cloud-scale dynamics, sophisticated microphysical processes, and explicit radiative-convective interaction (e.g., Tao and Simpson 1993; Tao et al. 1999; Shie et al. 2003). The 1999 Kwajalein Atoll field experiment (KWAJEX), one of several major TRMM (Tropical Rainfall Measuring Mission) field experiments, has successfully obtained a wealth of information and observational data on tropical convective systems over the western Central Pacific region. In this paper, clouds and convective systems that developed during three active periods (Aug 7-12, Aug 17-21, and Aug 29-Sep 13) around Kwajalein Atoll site are simulated using both 2D and 3D Goddard Cumulus Ensemble (GCE) models.

Both 2D and 3D simulated rainfall amounts and their stratiform contribution as well as the temperature, water vapor, and moist static energy budgets are examined for these three convective episodes. The modeled precipitation and apparent heat/moisture source/sink (Q1/Q2) are also validated by radar and sounding observations. Other interesting features involving the modeled hydrometeors, as well as CFAD (Contoured Frequency with Altitude Diagram) of modeled reflectivity and vertical velocity will also be presented in the meeting.

2. MODEL

The 2D or 3D GCE model used in this study is an anelastic, nonhydrostatic model that has been broadly used to study cloud-radiation interaction, cloud-environment interaction, and air-sea interaction. The cloud microphysics include a two-category liquid water scheme (cloud water and rain), and a three-category ice microphysics scheme (cloud ice, snow and hail/graupel). The model also includes solar and longwave radiative transfer processes, and a subgrid-scale turbulence (one-and-a-half order of turbulent kinetic energy) scheme. A stretched vertical coordinate with finer/coarser grid resolution in the lower/upper layers as well as a uniform horizontal coordinate with cyclic boundary conditions is included in the model. The

sounding derived large-scale temperature and moisture tendencies are imposed as the major forcing that drives the model. The model structure was detailed in Tao and Simpson (1993).

3. RESULTS

Figure 1 shows the time sequence of both 2D and 3D modeled domain-average surface rainfall rate and the observed surface precipitation (see details in figure caption). The temporal variation of both 2D and 3D modeled rainfall has agreed fairly well with the observation that was diagnostically estimated from the combined radar and raingauge data. Such a good agreement, we believe, is mainly attributed to the driving forcing -- the sounding derived large-scale temperature and moisture tendencies that were implemented into the model. However, both 2D and 3D simulated rainfalls have quantitatively shown a slight wet bias in all three episodes (also see Table 1). Overall, the 3D model has a slightly better performance than the 2D model in simulating both temporal evolution and total amount of rainfall. It is also shown in Table 1 that the 2D model generates more stratiform-type rainfall, while the 3D model significantly favors convective-type rainfall. The commonly found larger vertical velocity (not shown) in the 3D simulations may account for this interesting feature. Moreover, based on the 3D model results, the clouds and cloud systems are generally unorganized and short lived in the KWAJEX episodes. This numerical finding has further been validated by radar observations that will be presented in the meeting.

Evolutions of the 2D modeled domain-average apparent heat source (Q1) and the sounding estimate for the August 7-12, 1999 episode are shown in Figure 2. The modeled Q1 qualitatively agrees well with the observed Q1 over the entire model domain (Figure 2a and 2b, respectively), as well as captures the typical convective (Figure 2c) and stratiform (Figure 2d) Q1 structures discussed in previous studies (e.g., Houze 1997). Accordingly, a sole maximum heating is found around 500-550 mb in the convective profiles, while a maximum heating/cooling occurs in the upper (around 400mb)/lower (below the melting level) troposphere. A similar feature is also found in the other two episodes. On the other hand, the model simulations (Figure 3) also reasonably capture the typical structures of apparent moisture sink (Q2).

Table 2 lists the temperature, water vapor and static energy budgets of three episodes for both 2D and 3D model simulations. Regardless of the dimension, for all three episodes, the large-scale forcing and net condensation (sum of condensation, deposition, evaporation, sublimation, freezing, and melting of cloud) are the two major physical processes that account for the evolution of the budgets with surface latent heat flux and net radiation (solar and long-wave radiation) being secondary processes. Quantitative budget differences between 2D and 3D as well as between various episodes will be further discussed in the meeting. Modeled radar signatures (such as CFAD of reflectivity and vertical velocity) from the three simulations will also be presented in the meeting.

4. SUMMARY

The GCE-model (both 2D and 3D) results have reasonably captured several observed precipitation characteristics. The simulated rainfall temporal variation agrees fairly well with the sounding estimate. However, both 2D and 3D simulated rainfalls have shown a slight wet bias while the latter slightly dominates the former in rainfall simulation performance. More stratiform-type rainfall is found in the 2D

simulations while stronger vertical velocity occurs in the 3D simulations. The modeled Q1/Q2 qualitatively agrees well with the observed counterpart for both convective and stratiform regions.

5. REFERENCES

Houze, R. A., Jr., 1977: Structure and dynamics of a tropical squall-line system. *Mon. Wea. Rev.*, **105**, 1540-1567.

Shie, C.-L., W.-K. Tao, J. Simpson and C.-H. Sui, 2003: Quasi-equilibrium states in the tropics simulated by a cloud-resolving model. Part 1: Specific features and budget analyses, *J. Climate*, **16**, 817-833.

Tao, W.-K. and J. Simpson, 1993: The Goddard Cumulus Ensemble Model. Part I: Model description. *Terr. Atmos. Oceanic Sci.*, **4**, 35-72.

Tao, W.-K., J. Simpson, C.-H. Sui, C.-L. Shie, B. Zhou, K. M. Lau, and M. Moncrieff, 1999: Equilibrium states simulated by cloud-resolving models. *J. Atmos. Sci.*, **56**, 3128-3139.

Table 1. Domain-average surface rainfall amount (mm day⁻¹) and stratiform percentage (%) of three KWAJEX episodes for both 2-D and 3-D model simulations, along with the respective rainfall observations (mm day⁻¹).

	2-D Rainfall / Stratiform	3-D Rainfall / Stratiform	Rainfall Observations
Aug 7-Aug 12 1999	13.19 / 43.5	13.65 / 32.4	12.00
Aug 17-Aug 21 1999	12.94 / 43.3	12.85 / 31.3	11.06
Aug 29-Sep 13 1999	9.24 / 47.3	9.89 / 36.2	8.85

Table 2. (a) Temperature (C day⁻¹), (b) water vapor (mm day⁻¹), and (c) static energy (W m⁻²) budgets of three KWAJEX episodes for both 2D and 3D model simulations. Net condensation is the sum of condensation, deposition, evaporation, sublimation, freezing, and melting of cloud. The first and third columns contain the local time change and imposed large-scale advective tendency of the respective quantity. The net radiative contribution of short wave heating and long wave cooling is shown in the fourth column of Table 2a.

(a)

2-D / 3-D	dT/dt (C day ⁻¹)	Net Condensation	Large-scale Forcing	Net Q _R	Sensible Heat Fluxes
Aug 7-Aug 12 1999	-0.72 / -0.80	3.47 / 3.54	-3.19 / -3.19	-1.07 / -1.25	0.08 / 0.10
Aug 17-Aug 21 1999	-0.37 / -0.68	3.32 / 3.25	-2.84 / -2.84	-0.91 / -1.17	0.06 / 0.08
Aug 29-Sep 13 1999	-0.29 / -0.43	2.37 / 2.50	-1.98 / -1.98	-0.78 / -1.08	0.10 / 0.14

(b)

2-D / 3-D	d(Q _v) / dt (mm day ⁻¹)	Net Condensation	Large-scale Forcing	Latent Heat Fluxes
Aug 7-Aug 12 1999	-1.88 / -2.32	-13.50 / -13.95	9.61 / 9.61	2.01 / 2.03
Aug 17-Aug 21 1999	-5.34 / -5.13	-12.95 / -12.85	6.08 / 6.08	1.54 / 1.64
Aug 29-Sep 13 1999	-1.89 / -2.15	-9.24 / -9.89	4.84 / 4.96	2.51 / 2.78

(c)

2-D / 3-D	D(C _p T+LvQ _v) (W m ⁻²)	Net Condensation	Large-scale Forcing	Net Q _R	Sensible Heat Fluxes	Latent Heat Fluxes
Aug 7-Aug 12 1999	-136.3 / -158.9	5.58 / 0.79	-87.1 / -87.1	-121.9/-142.9	9.04 / 11.68	58.13 / 58.77
Aug 17-Aug 21 1999	-197.1 / -225.8	4.37 / 0.00	-148.6/-148.6	-103.6/-133.8	6.31 / 9.16	44.43 / 47.43
Aug 29-Sep 13 1999	-87.5 / -110.8	4.11 / 0.01	-86.1 / -83.4	-89.5/-124.0	11.22 / 16.06	72.76 / 80.48

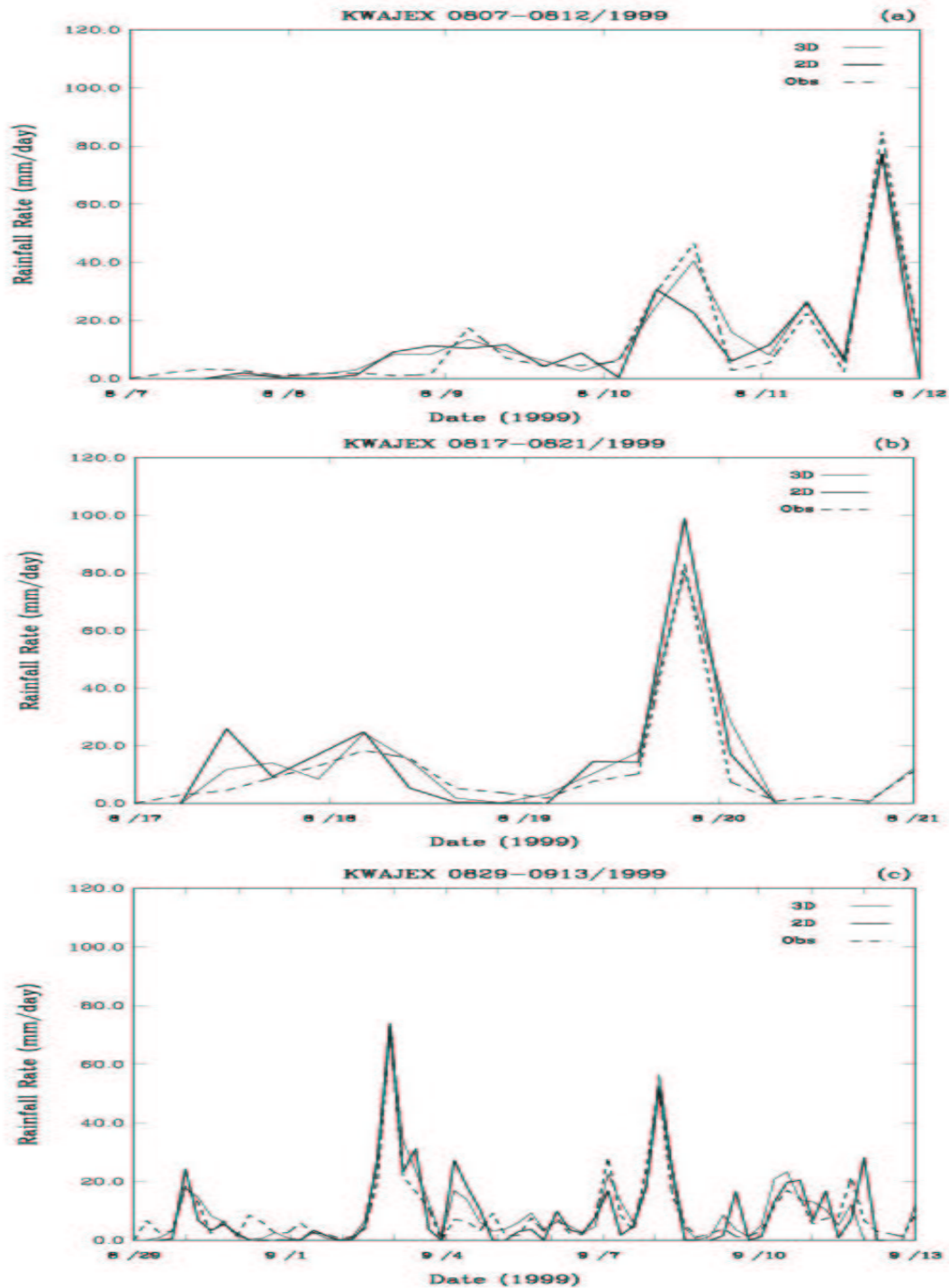


Figure 1. Time series of the 2D (thick solid line), 3D (thin solid line) modeled, and the observed (dashed line) domain-average surface rainfall rate (mm day^{-1}) for (a) August 7-12, (b) August 17-21, and (c) August 29-September 13 1999. The observed surface rainfall shown here was based on the six-hour-bin combined radar and raingauge data (provided by Zhang et al. at State University of New York, Stony Brook).

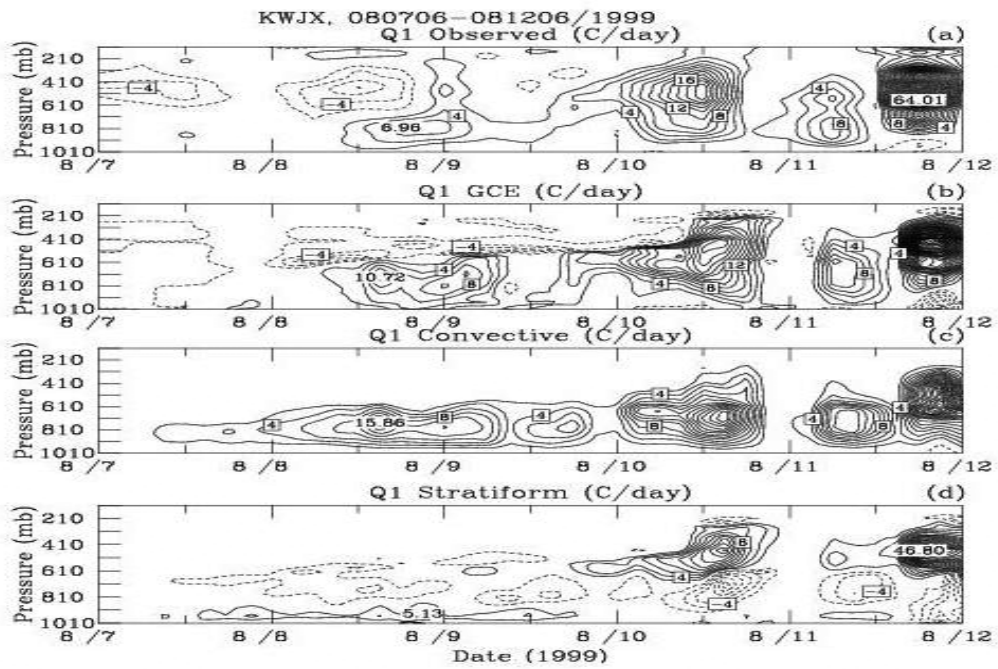


Figure 2. Evolution of the 2D domain-average apparent heat source (Q1) for the August 7-12, 1999 episode, (a) derived diagnostically from soundings (provided by Zhang et al. at State University of New York, Stony Brook), and simulated from the GCE model over (b) the entire region, (c) the convective region, and (d) the stratiform region. The contour interval is 2 C day⁻¹ for each panel.

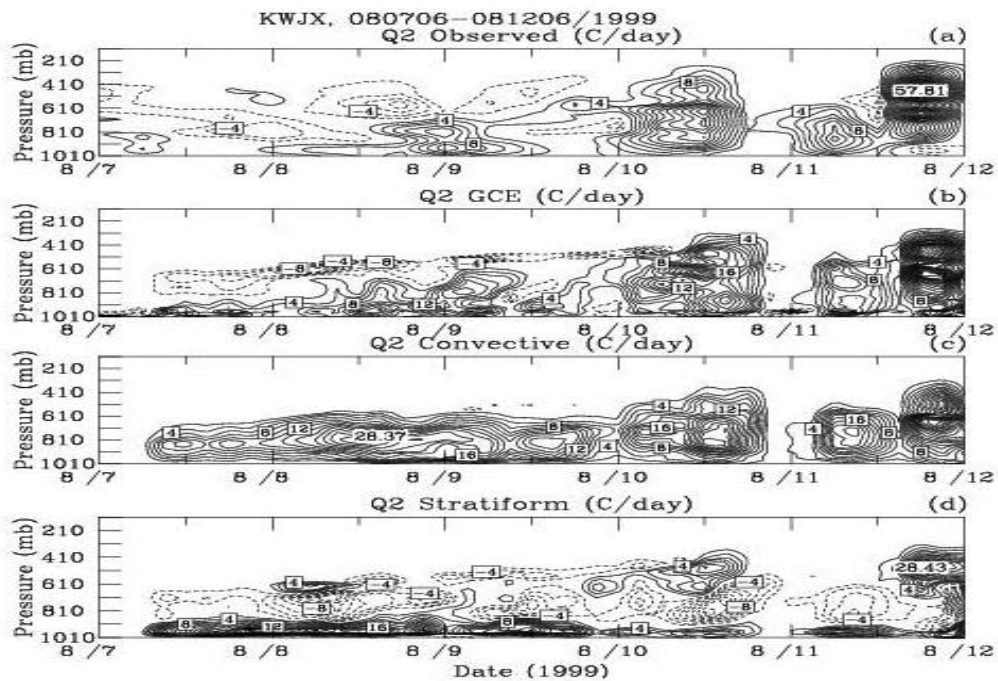


Figure 3. Same as Figure 2 except for the moisture (Q2) budget.